

PCCP

Accepted Manuscript



This is an *Accepted Manuscript*, which has been through the Royal Society of Chemistry peer review process and has been accepted for publication.

Accepted Manuscripts are published online shortly after acceptance, before technical editing, formatting and proof reading. Using this free service, authors can make their results available to the community, in citable form, before we publish the edited article. We will replace this *Accepted Manuscript* with the edited and formatted *Advance Article* as soon as it is available.

You can find more information about *Accepted Manuscripts* in the [Information for Authors](#).

Please note that technical editing may introduce minor changes to the text and/or graphics, which may alter content. The journal's standard [Terms & Conditions](#) and the [Ethical guidelines](#) still apply. In no event shall the Royal Society of Chemistry be held responsible for any errors or omissions in this *Accepted Manuscript* or any consequences arising from the use of any information it contains.



Journal Name

ARTICLE

Enhanced Surface Hydrophilicity of Thin-film Composite Membranes for Nanofiltration: A Experiment and DFT Study

Zhiwei Lv, Jiahui Hu, Xuan Zhang* and Lianjun Wang*

Received 00th January 20xx,
Accepted 00th January 20xx

DOI: 10.1039/x0xx00000x

www.rsc.org/

In the current study, thin-film composite (TFC) nanofiltration membranes desirable for water softening were successfully developed through interfacial polymerization using N-(2-hydroxyethyl)ethylenediamine (HEDA) as the amine monomer in aqueous phase. The hydrophilicity of the membrane surface was greatly enhanced with the introduction of the residual hydroxyl groups during the fabrication process. The TFC membranes possessed a permeate flux of 15.8 L/m²h under 0.6 MPa, with a rejection of 85.9%, 73.8%, 99.8% for Na₂SO₄, MgSO₄ and Congo red, respectively. The interplays of the solvent, solute and polymer matrix on the separation performance were investigated by means of solubility parameters study. Moreover, density functional theory was employed to calculate the Fukui function by the Hirshfeld charge, which gave the global and local softness value to predict the reactivity of the atomic sites in the HEDA molecule. The findings of this study support the possible forming mechanism of the barrier layer by the density functional theory for the first time. The TFC membrane was found to be stable and displayed a good separation ability over a week-long filtration process. The combined results of this work suggest that these HEDA/TMC TFC nanofiltration membranes are promising candidates for various applications, such as desalination and dye removal from wastewater.

Keywords: Thin-film composite nanofiltration membrane; Polyamide; Interfacial polymerization; Density functional theory; Fukui function

Introduction

Pressure driven nanofiltration (NF) through membranes is a widely accepted process due to its many advantages such as lower operational pressure and cost.¹⁻⁵ NF is a membrane separation process between reverse osmosis and ultrafiltration, with a molecular weight cut off ranging from 200 to 1000 Da⁶ and applied in many fields such as removal of contaminants from groundwater, softness of surface water and treatment of wastewater.⁷⁻⁹ Generally, NF membranes are prepared by various methods such as interfacial polymerization (IP), nanoparticles incorporation, and ultraviolet treatment, *etc.*¹⁰⁻¹² Among them, the most widely used method for preparation of thin-film composite (TFC) membranes is the IP technique.¹³⁻¹⁵ The barrier layer and the support membrane in this technique have been already optimized according to different conditions.¹⁶⁻¹⁷ To date, most studies have been focused on the polyamide-based (PA) NF membrane due to its wide pH operating conditions as well as good chemical stability.^{2,3,4,10,18} However, the hydrophilicity of the PA membrane mainly depends on the amount of carboxylic acid groups resulting from

the hydrolysis of benzoyl chloride groups. Further improvement of the PA membrane described above in terms of better water permeability and lower energy consumption appears to be difficult. Therefore, it is essential to investigate other modifications to enhance the hydrophilicity of PA membranes.

It is well-known that membranes containing hydroxyl groups can improve surface hydrophilicity. A novel polyester composite membrane has been prepared from triethanolamine (TEOA) and trimesoyl chloride (TMC).¹⁹ The water flux of this membrane reached to 11.5 L/m² h and its rejection of Na₂SO₄ was improved to 82.2%, at pH 3.0 in the feed. Thus, this is quite a promising membrane for further investigations. Recently, Zhao *et al.* developed a series of dopamine/TMC composite membranes. The resulting membranes showed a pure water flux of 13.7 L/m² h and a Na₂SO₄ rejection of 63.8% due to their special molecular structure and adsorption function.²⁰ Considering the requirements of industrial scale-up and costs, the use of functional monomers and precursors having complicated syntheses is not very feasible.

Due to the importance of materials selection, it is essential to design a careful and purposeful experimental investigation. Until now, most of the NF related studies have been focused on the separation performance, *i.e.*, the permeate flux and rejection properties. However, to date, the relationship between primary structure of polymers and membrane properties has not yet been investigated properly. From a chemistry viewpoint, it is useful for this structure-property relationship to be addressed

^a Key Laboratory of Jiangsu Province for Chemical Pollution Control and Resources Reuse, Nanjing University of Science & Technology, Nanjing 210094, China.

† Footnotes relating to the title and/or authors should appear here.

Electronic Supplementary Information (ESI) available: [TFC membrane fabrication condition]. See DOI: 10.1039/x0xx00000x

and extensively studied. Recently, density functional theory (DFT) has been applied to investigate the “atomic world” based on quantum chemistry principles, and thus has drawn much attention.²¹⁻²³ For instance, a comparison study was performed between two kinds of nanofiltration membranes (NE90 and NE70) to confirm the natural organic matter removals. The results showed that the carboxylic compound has higher energy gap and tend to adsorb on the membrane surface than the other compounds (phenolic and acetic acid). Therefore, the use of NE90 for organic compound rejection has to be faced with fouling problems due to its greater bound energy than NE70.²¹ Lo *et al.* calculated the global/local reactivity of piperazine (PIP) and *m*-phenylenediamine (MPDA) molecules towards TMC with DFT. It was found that the reaction between MPDA and TMC for the preparation of TFC membrane would be much facile compared to the case of PIP with TMC, since there would be more unreacted acyl carboxylic groups left which produce more charges on the surface, and thus leads to the better selectivity of bivalent salt rejection for the latter.²² More recently, DFT and average local ionization potential energy were employed to show the lowest energy conformations polyethylene glycol (PEG) precursors derived from different amine terminated molecules. All the PEGylated TFC membranes exhibited almost similar performance and good antifouling property owing to their closer reactivity of the amine groups towards TMC.²³ In general, the scale of a quantum simulation method makes it facile to examine the interactions among various small molecules, *e.g.*, salt ions, organic solutes, functional groups in polymer matrix, *etc.* Thus, there exists a possibility to explore the thin-film forming mechanism with regard to the reactivity discrepancies of the reactants, so that the detailed information during an IP process might be obtained. However, to date, the useful data on this research field are still rather limited.

In this work towards developing new and improved TFC membranes, a commercially available monomer, *N*-(2-hydroxyethyl)ethylenediamine (HEDA) was chosen due to its low cost and environmentally friendly properties. Due to the presence of the aliphatic amine and hydroxyl groups, it is expected that the monomers would be obtained with good reactivity in facilitating the IP process. A series of TFC membranes were prepared by the interfacial polymerization of HEDA and TMC on a polysulfone porous substrate. The separation properties of these membranes were then evaluated by determination of the permeate flux and rejection of salts and dye solutions. Furthermore, the quantum mechanical simulation was also investigated to determine the reactive sites of HEDA monomer based on DFT theory. By comparing the Hirschfield charge, together with their pK_a values, brief information on the reactivity sequence could be obtained. Based on this finding, a new active layer forming mechanism was put forward with regard to our HEDA/TMC system.

Materials

Flat sheet polysulfone ultrafiltration membranes with a molecular weight cut-off (MWCO) of around 35,000 Da were

provided by Hangzhou Water Treatment Technology Development Center Co. Ltd and used as a support membrane. 1,3,5-Benzenetricarboxylic chloride (TMC, purity>98%) was obtained from Meryer Chemical Reagent Co. Ltd. (Shanghai, China). *N*-(2-hydroxyethyl)ethylenediamine (HEDA) was purchased from Aladdin Industrial Corporation (Shanghai, China). De-ionized water used in the experiments was purified using Millipore water purification with a minimum resistance of 18 M Ω . Inorganic salts MgSO₄ and Na₂SO₄ and organic dye of Congo red (CR) and Rhodamine B (RB) of analytical grade were used as the model solutes to investigate the performance of the HEDA/TMC composite membranes. All reagents and solvents were used without further purification.

Preparation of TFC membrane

The HEDA/TMC TFC membranes were prepared via the interfacial polymerization technique on the PSF porous support membrane in an assembly clean room and the process was described as follows. Firstly, the pH of aqueous solution containing different concentration of 0.3 - 0.7% HEDA was adjusted to 11 with NaOH, and then the solution was poured onto the surface of polysulfone substrate and allowed to keep at least 3 min. Afterwards, the excess solution was removed from the surface of support membrane, and membrane was air-dried and tissue off at room temperature until no liquid drop remained. The amine saturated membrane was soaked by organic solution with a certain amount of TMC ranging from 0.05 - 0.25% (w/v) and *n*-hexane for 2 min, and then dried in a hot air oven at 60 °C for 5 min for further thermal treatment. Finally, the resulting membrane was washed by de-ionized water and stored wetly until it was tested.

Characterization of TFC membrane

Attenuated Total Reflection Fourier transformed Infrared Spectroscopy (ATR-FTIR) was used to evaluate the functional groups of TFC membrane surface. The ATR-FTIR spectra were obtained via Nicolet IS-10 spectrometer equipped DTGS detector with a 4 cm⁻¹ spectra resolution at room temperature. Field emission scanning electron microscopy (FE-SEM, FEI Quant 250FEG, USA) was employed to investigate the surface and cross-section images of TFC membranes.

Surface chemical composition of HEDA/TMC TFC membranes was characterized by X-ray photoelectron spectra (XPS, PHI Quantera II, Japan). The samples were mounted on the holder and then transferred to the analyzer chamber. Measure spectra of the samples were recorded via the AugerScan 3.21 software ranging from 0 eV to 1100 eV.

Atomic force microscopy (AFM, Mutilmode8, German) was used to measure the surface morphology of the polyamide membranes. AFM measurement (Intelligent mode) was carried out in air at room temperature and 5×5 μ m area was scanned. Silicon tips (NSG10, NT-MDT) with a resonance frequency of *ca.* 330 kHz were employed.

Thin-film composite membranes performance evaluation

The permeate flux and rejection were evaluated with laboratory-scale cross-flow membrane equipment having an effective membrane area of 12.56 cm². Membranes were pretreated at a trans-membrane pressure of 0.6 MPa at least 30 min to reach a steady state before measurement. The permeate flux was obtained by measuring the weight of permeability at 25 °C and calculated according the following Equation (1):

$$F = \frac{W}{At} \quad (1)$$

where W is the total weight of permeated pure water, A represents the effective membrane area, and t denotes the filtration time.

The rejection rate was determined by measuring the conductivity of salt solution with Na₂SO₄ of 1 g/L and MgSO₄ of 1 g/L and the absorbance of dye solution consisted of 0.1 g/L. The rejection rate was defined by the following Equation (2):

$$R = \left(1 - \frac{C_p}{C_f}\right) \times 100\% \quad (2)$$

where C_p and C_f refer to the concentration of the feed and the permeate, respectively. The salt concentration was determined by the electrical conductivity of the corresponding salt solution using an electrical conductivity (UT30B, Shenzhen Uni-trend Electronics Company), while the concentration of Congo red solution was evaluated by an ultraviolet spectrophotometer (Lambda 25, UV/VIS Spectrometer, USA).

Surface Zeta potential measurement

Streaming potential was measured via a self-assembled setup. Reversible Ag/AgCl electrodes, placed on the two sides of the membrane, were used to evaluate the resulting electrical potential (ΔE) as the trans-membrane pressure differential (ΔP) changed ranging from 0 to 0.12 MPa. The streaming potential (SP) was calculated according to the formula: $SP = \Delta E / \Delta P$. Measurement was carried out with 0.01 mol/L KCl solution under 3.0 - 9.0 pH conditions adjusted by hydrochloric acid and potassium hydroxide solution. Zeta potential (ζ) was determined by the Helmholtz-Smoluchowski Equation (3):

$$\frac{\Delta E}{\Delta P} = \frac{D\zeta}{\mu k_m} \quad (3)$$

where D is the dielectric permittivity, and μ and k_m are the viscosity and the conductivity of the solution, respectively.²⁴

Computational methods

Calculations were carried out for HEDA molecule with the density functional theory by using Becke's three-parameter hybrid functional with correlation formula of Lee, Yang, and Parr (B3LYP). The geometry was optimized at B3LYP/DNP level of theory in aqueous phase. The hybrid density functional (B3LYP) and the double numerical with dynamic nuclear polarization (DNP) basis set within the DFT was carried out by the software package DMol3 in Material Studio (MS) of Accelrys Inc. The local softness was also investigated to predict the local reactivity.

In this study, the local softness, $s(r)$, was calculated by the Equation (4):

$$s(r) = Sf(r) \\ s^-(r) = Sf^-(r)$$

In this paper, s^- refers to the local softness of nitrogen or oxygen atom of HEDA molecule. This function was defined as the charge as the change in electron density at a given atomic site with change in number of electrons at a constant nuclear geometry. It showed the tendency of the electronic density to distort at a given position to accept or donate electrons. It pointed out the most reactive sites in a given molecule. The site with large Fukui function was regarded as soft center. In contrast, the site with a small Fukui function was hard center. The maximum value of Fukui function indicated the most reactive site in a molecule. Fukui function, $f(r)$, was calculated by the Hirschfield charge with DMol3. There were three different kinds of $f(r)$ to determine a nucleophilic, electrophilic, or radical attack.

$$f^-(r) \text{ for electrophilic attack (acts as a nucleophile)} \\ f^+(r) \text{ for nucleophilic attack (acts as an electrophile)} \\ f^0(r) \text{ for radical attack} \quad (4)$$

The global softness S was expressed by the Equation (5) from the finite difference approximation,

$$S = \frac{1}{I - EA} \quad (5)$$

where I and EA denoted the ionization energy and the electron affinity, respectively. To calculate global softness, EA and I approximated the highest occupied molecular orbital (HOMO) and the lowest unoccupied molecular orbital (LUMO) in terms of the Koopman's theorem, respectively. Therefore, the global softness could be expressed as the Equation (6):

$$S = \frac{1}{E_{LUMO} - E_{HOMO}} \quad (6)$$

In the study, $s^-(r)$ refer to the local softness of nitrogen and oxygen atom of the monomer, indicating the reactivity of the atom site.

The solubility parameters were calculated via atomistic molecular dynamics simulation (Forcite module) using the COMPASSII force field, which is an ab initio force field optimized for condensed-phase systems. To arrive at the initial packing, 100 molecules (CR or RB) were simulated in a cubic unit cell with 3D periodic boundary conditions at 298 K. After geometric optimization, the unit cell was equilibrated by the annealing dynamics simulation method, which included five cycles of NVT ensemble dynamics between 300 and 800 K to prevent the system from being trapped in a local minimum. After reaching the lowest energy configuration, 1000 ps of thermalizing NPT dynamics (1 fs time step) was performed to reach the actual system temperature and pressure. Next, the cohesive energy density (CED) was determined by sampling the system and collecting data for final 500 ps. The solubility parameter was calculated from CED, by Equation (7):

$$\delta_i = \left(\frac{\sum E_{coh}}{\sum V_m} \right)^{1/2} = (CED)^{1/2} \quad (7)$$

where ΔE_{coh} and V_m are the cohesive energy and molar volume of the input molecules, respectively.

Results and Discussion

The nomenclature used for the series of TFC membranes is: XaYb, where X and a stand for HEDA and its concentration in an aqueous phase, respectively; Y and b refer to TMC and its concentration in an organic phase, respectively.

To optimize the IP procedure, membrane curing temperature and thermal period tests were prior carried out, and the final condition was set at 60 °C for 5 min (see Fig. S1 and Fig. S2).

Chemical composition and morphology of TFC membrane

Table 1 Surface atomic composition of the barrier layer

| | C% | N% | O% | O/N |
|--------------------|-------|-------|-------|------|
| Total cross-linked | 65.38 | 15.30 | 19.23 | 1.25 |
| Linear polymer | 65.00 | 10.00 | 25.00 | 2.50 |
| X0.5Y0.1 | 68.50 | 11.00 | 20.50 | 1.86 |

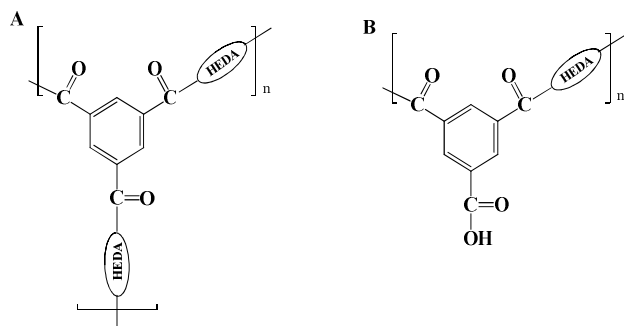


Fig. 1 The chemical structure of polyamide from and TMC and HEDA contains A (Total cross-linked) and B (Linear) polymer repeating units.

The two possible cross linking structure of the TFC membranes surface was shown in Fig. 1. Elemental compositions of the TFC membranes containing carbon (C), oxygen (O), and nitrogen (N) are listed in Table 1. Theoretically, the O/N ratio should be 1.25 for a completely cross-linked structure, and 2.5 for a linear structure. The experimental O/N ratio was found to be 1.86 for the membrane X0.5Y0.1, which is closer to the value 1.25 for a completely cross-linked structure, thus indicating a formation of a tight and compact structure on the surface.

Water treatment performance of TFC membrane

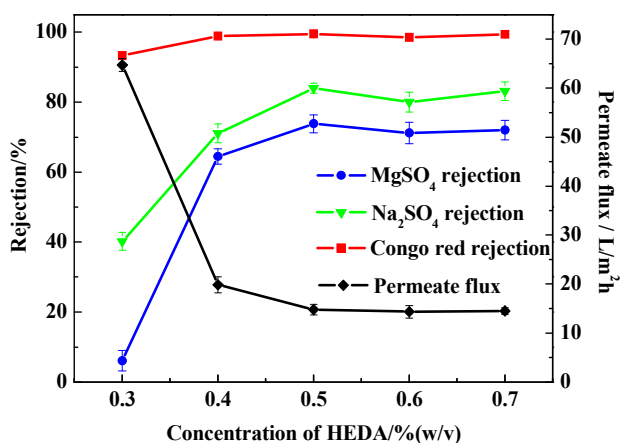


Fig. 2 Effect of HEDA concentration on the permeate flux and rejection (Condition: HEDA 0.3 – 0.7% (w/v), TMC 0.1% (w/v), salt concentration 1.0 g/L, Congo red 0.1 g/L, 0.6 MPa).

Fig. 2 shows the effects of increasing concentrations of HEDA on the rejection and the permeate properties of the TFC polyamide membranes at a fixed TMC concentration of 0.1% (w/v) under 0.6 MPa. Actually, the model interfacial polymerization in a flask was initially carried out with HEDA concentration starting from 0.1 – 0.2% (w/v). However, rather loose polymer was obtained and could not be pulled from the interface. Applying this condition to the membrane fabrication only resulted in a negligible salt rejection. Therefore, the threshold concentration of HEDA was chosen as 0.3% (w/v), where a medium rejection of 40% to Na₂SO₄ was found. It can be seen that the rejection of Na₂SO₄ and MgSO₄ increases considerably by increasing the concentration of HEDA from 0.3% to 0.4%, while the rejection remains constant with further increase in concentration from 0.4% to 0.7%. On the other hand, the permeate flux of the TFC membranes decreases with increasing concentration of HEDA. The highest rejection abilities observed are 85.9% and 73.8% for Na₂SO₄ and MgSO₄, respectively, with the feed concentration of 0.5% (w/v) HEDA, while maintaining the permeate flux as high as 15.8 L/m²h. Congo red with a molecular weight of 699 g/mol is entirely rejected (99.8%). Compared to some other similar TFC membranes which were prepared from ethyl diamine and TMC,²⁵ the X0.5Y0.1 showed improved water flux and Na₂SO₄ rejection, indicating the enhanced hydrophilicity and negatively charged surface with the aid of “-OH” introduction. In order to further confirm the surface property, contact angle measurement was performed for X0.5Y0.1. It exhibited a low value of 64.6 ± 1.2 degree than the virgin substrate of 78.5 degree, which agrees our speculation. Furthermore, the relationship between filtration performance and the thickness and density of the barrier layer has been studied by Duan and Yu.^{26,27} The interfacial polymerization on the substrate process typically consists of an initial fast stage and a second slow growth stage.²⁸ This behavior is seen in our experiments as well. The initial fast reaction in the interfacial zone between two immiscible solutions forms a nascent membrane with a large free volume and a loose structure in the initial stage, which

results in high flux and low rejection. As the reaction progresses, the HEDA molecules in the aqueous phase diffuse into the organic phase through the nascent membrane. The rate of this diffusion process is slow due to the low permeability of the nascent membrane. With further progress of the polymerization reaction, the nascent membrane becomes thicker and denser to form a tight and compact barrier layer, which displays higher rejection and lower permeate flux. Compared to the higher rejection of Na_2SO_4 , the relatively lower rejection of MgSO_4 is mainly due to the multivalent Mg^{2+} positive ions in the feed, which “shield” the negative charges on the membrane surface as a result of a weakened Donnan effect.²⁹

Having checked the separation characteristics of the TFC membranes, it was quite essential to further understand the relationship between the solvent, solute and membrane surface properties. Here we chose RB (flux of $18.6 \text{ L/m}^2\text{h}$; rejection of 75.6%) and CR (flux of $15.8 \text{ L/m}^2\text{h}$; rejection of 99.8%) as the two typical examples, and the solubility parameter values are listed in Table S1. Generally, the solute tends to pass through the membrane matrix easier when the solute had a higher affinity to the membrane matrix than the solvent.^{30,31} Since the dye solutes used in this study were in the same condition (both in water aqueous solution), the difference is mainly on their δ values to the polymer. It was found that the δ between the CR and polymer ($|\delta_1 - \delta_{\text{polymer}}| = 10.7 \text{ (J/cm}^3)^{1/2}$) was greater than that of RB to polymer ($|\delta_2 - \delta_{\text{polymer}}| = 3.8 \text{ (J/cm}^3)^{1/2}$), which indicating the higher solute affinity and an enriched permeate for the latter ($15.8 \text{ L/m}^2\text{h}$ for CR and $18.6 \text{ L/m}^2\text{h}$ for RB). From another aspect, it should also be mentioned that a higher solute-solvent affinity would lead to a lower rejection. The difference between solubility parameters of CR and water ($11.3 \text{ (J/cm}^3)^{1/2}$) is lower than that of RB and water ($18.2 \text{ (J/cm}^3)^{1/2}$), which should result in a lower rejection of former. However, the experiment result was just the opposite, that is, a higher rejection of 99.8% for CR compared to 75.6% for RB. The phenomenon might be attributed to the charge effect which predominantly determine the rejection rate. CR, as a negatively charged molecule, is more easily to be rejected due to the relatively strong repulsion to the membrane surface.

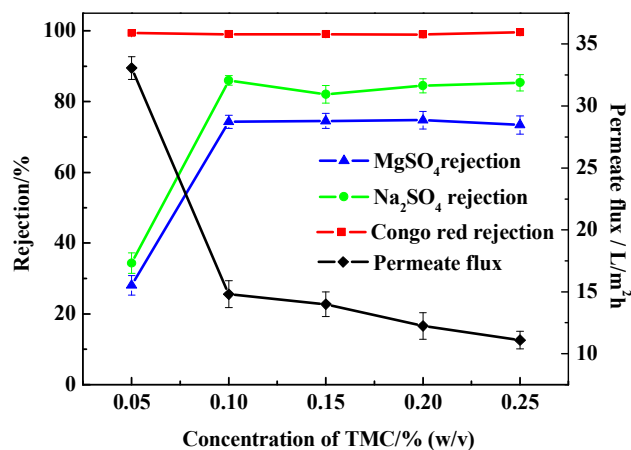


Fig. 3 Effect of TMC concentration on the permeate flux and rejection (Condition: HEDA 0.5 (w/v), TMC 0.05- 0.25 % (w/v), salt concentration 1.0 g/L, Congo red 0.1 g/L, 0.6 MPa).

The effect of increasing concentration ranging from 0.05% (w/v) to 0.25% (w/v) of TMC in the organic phase on the rejection and permeate flux properties of TFC membranes is shown in Fig.3. It was seen that at very low concentration of TMC (0.05% (w/v)), the membrane showed rather low salt rejection, which was probably attributed to the low degree of cross-linking. The membrane only formed a thin and loose barrier layer under this condition. When the TMC concentration is increased to 0.1% (w/v), a thicker and more compact polyamide barrier layer is formed which is able to more effectively reject inorganic salts and dye in the HEDA/TMC composite membranes. Further increase in TMC concentration from 0.1% (w/v) to 0.2% (w/v), the highest values of rejection and permeate flux is displayed. The rejection of Na_2SO_4 is almost constant as the concentration of TMC is increased from 0.1% (w/v) to 0.2% (w/v). This properties improved of filtration can be attributed to the increase thickness and degree of cross-linking of the barrier layer in the slow growth stage.

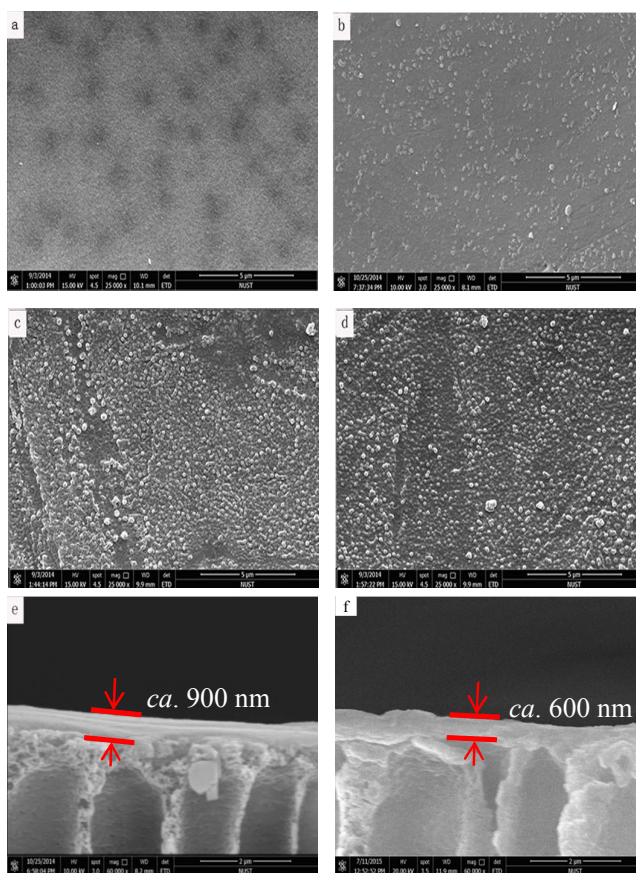


Fig. 4 SEM surface and cross-section images of the resulting membrane (25,000X): (a)PSF substrate; (b) X0.3Y0.1; (c) X0.5Y0.1; (d) X0.5Y0.2; (f) PSF substrate(60,000X) (e)cross-section of X0.5Y0.1 (60,000X).

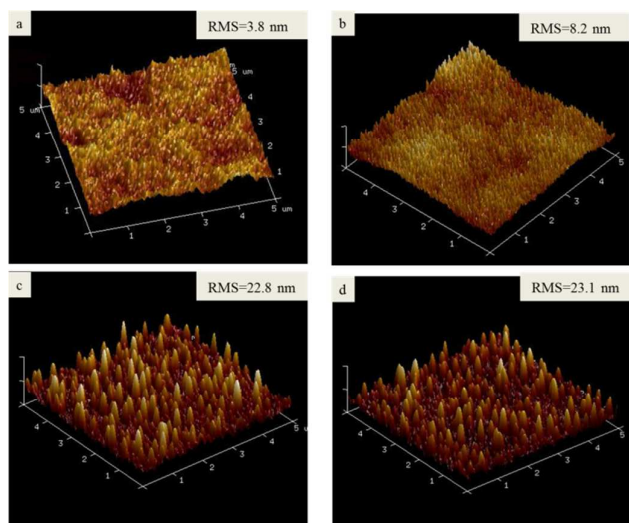


Fig. 5 Three-dimensional AFM images of the resulting membranes: (a) PSF substrate; (b) X0.3Y0.1; (c) X0.5Y0.1; (d) X0.5Y0.2.

The morphology of TFC membranes is characterized by FE-SEM, as shown in Fig.4. In the FE-SEM images, the white area represented the peaks and the black region denoted the valleys. Comparing Fig. 4 (a), (b) and (c), it can be seen that the nodular-like regions were gradually enhanced with increase in concentration of HEDA in the aqueous phase, suggesting the formation of compact surface structure and the presence of peak-and-valley characteristics. When combined with the data from Fig.3, we could deduce that the decreasing permeate flux was likely due to gradually narrowing pores as a result of increased cross-linking in the barrier layer. Furthermore, as shown in Fig. 4 (e), the upper barrier layer of the TFC membrane could be roughly estimated to be near 300 nm in thickness compared with the PSF substrate in Fig. 4 (f), which was very similar to the other reported literature.^{15,27,32,33}

Fig. 5 represents the data on the surface topographies of the polysulfone supporting membrane and the HEDA/TMC TFC membrane. The root-mean-square (RMS) height, defined as mean of the root of the distance from standard surface to indicated surface, was an important parameter in the AFM analysis. The roughness values increased in the order of $a < b < c < d$ with increase in the concentration of HEDA and TMC. It was worth noting that the rejections of salts or dye are improved with the increase in the roughness. This was likely due to the enhanced specific surface area which effectively increases the probability of contact between the negative charges ($-\text{COO}^-$) on the membrane surface and ions in the feed, and thus improved the rejection properties.

Zeta potential

Zeta potential curves of the HEDA/TMC composite membranes and PSF substrate as a function of pH values are shown in Fig. 6. The dissociation of the surface groups from the barrier layer was influenced by the pH of the solution in contact with the layer. The separation of salts or dye was largely dependent on

electrostatic repulsion arising from the interaction between negative charges on the surface of composite membranes and negative ions in the feed. The HEDA/TMC composite membranes possessed an amphoteric surface in the entire pH range with the isoelectric point at pH 6.0. The surface of HEDA/TMC composite membranes was found to be positively charged below pH 6.0 and negatively charged above this pH value due to the protonation of the amine group of HEDA and the formation of carboxylate anion, respectively.³⁴ Thus, it was likely that the multivalent ions would be effectively rejected in neutral conditions due to the negatively charged surface of our TFC membranes.

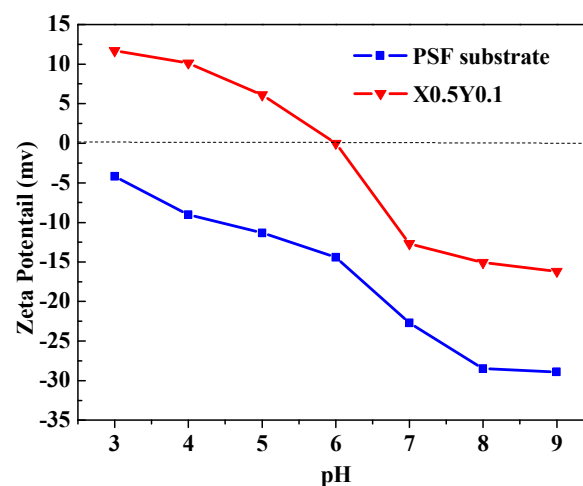


Fig. 6 The Zeta potential of X0.5Y0.1 and PSF substrate as a function of pH.

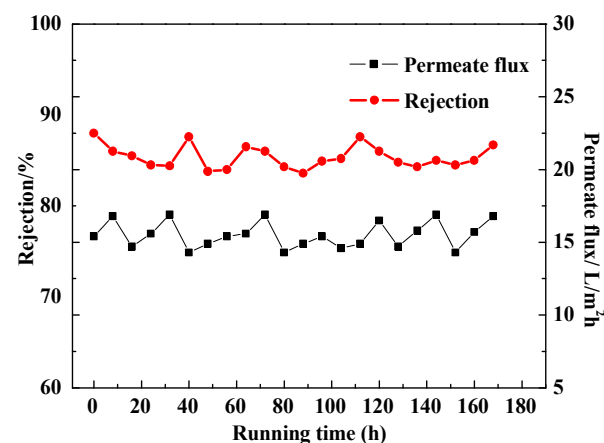


Fig. 7 Long-time stability test of TFC membrane (X0.5Y0.1). Testing condition: 0.6 MPa, 25 °C.

Long-time stability of TFC membrane

The stability and durability of nanofiltration composite membranes are important factors for filtration applications. Therefore, a long-term continuous test of the TFC membranes

was carried out with a feed of 1.0 g/L Na_2SO_4 at 0.6 MPa, as shown in Fig. 7. It can be seen that the TFC membrane exhibits good durability, with permeate flux and rejection properties remaining constant during the entire testing period at around 14.3 - 16.8 $\text{L}/\text{m}^2\text{h}$ and 83.6 - 87.6%, respectively.

Quantum chemistry Study

The optimized geometry and quantum dynamics of HEDA molecule is shown in Fig. 8. In terms of frontier orbital theory, the reaction between reactants takes place mainly at the highest occupied molecular orbital (HOMO) and lowest occupied molecular orbital (LUMO).³⁵ It can be seen that active reaction sites are located at the two nitrogen atoms and an oxygen atom in the HEDA molecule, as shown in Fig. 8 (b). To determine the most preferred site for nucleophilic attack, Hirshfeld charges were investigated to calculate the Fukui function ($f^-(r)$) in this study.

All the calculated data were found to be positive, indicating nucleophilicity of the three functional groups, i.e., $-\text{NH}_2$ (7N), $-\text{NH}-$ (4N) and $-\text{OH}$ (1O) group (Table 2). The higher the value for local softness, the higher is the reactivity for the site.²² Herein, the possible three react sites exhibited a reactivity sequence of $4\text{N} \gg 7\text{N} > 1\text{O}$. However, it is widely considered that a secondary amine always suffer from the steric hindrance effect which resulted in a dramatically reduced nucleophilicity. In order to further judge the competitive relationship among those three atoms, dissociation constant were investigated, where $\text{p}K_a$ is 10.84 - 10.98, 10.65 - 10.66 and 15.5 - 15.9 for diethylamine, ethylamine and ethanol.³⁶⁻³⁸ Combining with the aforementioned results, it is desired to see that 4N and 7N should be obtained higher reactivity than 1O atom under our IP condition at pH around 11.0. Therefore, the “Ar-CON(R₁)R₂” unit is instantaneously generated at the 4N site once the amine-saturated film is covered by the organic TMC solution. Initially, only a few dimers or trimers are formed due to the different reactivities. However, the loose nascent layer is unable to block further diffusion of the molecules. As a result, more and more HEDA monomers pass through and react continuously with the newly-formed oligomers without much resistance for a certain period. Meanwhile, it is well accepted to us that the polymerization proceeds with an irreversible coupling of monomers/oligomers and a deepening penetration of the organic solution. At some point, the polymer may gel out and the chain growth is presumably much slower or stopped.³⁹⁻⁴² In our case, the intermediates generated at the beginning might be very soluble in the organic phase due to their too small molecule weights, and thus the polymerization on a substrate would be processed in a homogenous state, which suggested the continuously increased molecular weight and the thickness of the polyamide layer. Additionally, although it is quite difficulty to dissociate the hydrogen from the aliphatic hydroxyl group, it might be still inevitable if there existed a little amount of “-OH” which participated in the polymerization since alkaline condition and a heating up operation were applied during the IP process. Therefore, a small “O=C=O” peak could be observed in the FTIR spectrum (1727 cm^{-1} in Fig.S3). It can be concluded

that the crosslinking degree was further increased due to the esterification. Even based on a small amount of the crosslinkable reactive sites, a denser and thicker active layer would form, which resulted in a sacrifice in water flux.

This proposed formation theory has a favorable effect on the performance of our TFC membranes. As the results indicate, all of the membranes show acceptable rejection rates for both salt and aqueous dye solutions; however, the water permeation ability is not as good as expected. The relatively low water flux is mainly due to the small pore sizes and the thickness of the barrier layer, as mentioned above. Fortunately, there still many hydroxyl groups remained after the membrane fabrication, as revealed by the contact angle results and a moderate improvement on the water flux (compared to the EDA type),²⁵ which suggested the enhancement in surface hydrophilicity. The dynamic simulation results provide a clear picture of the structure of the membranes. Monomers or polymers having multi-functional groups with similar reactivities are more likely to result in an instantaneous interfacial condensation.

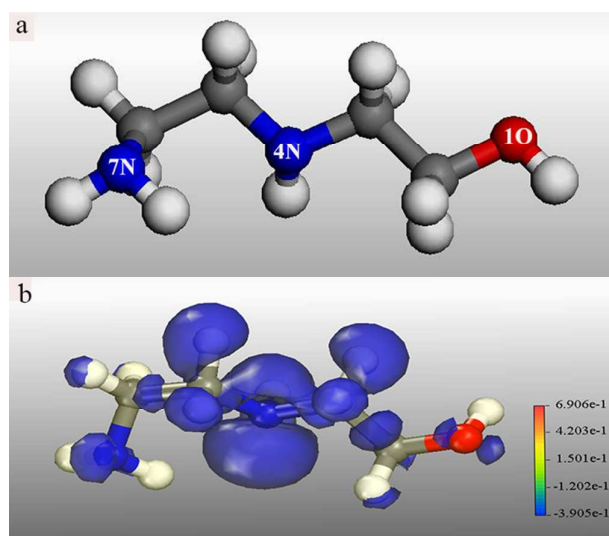


Fig. 8 B3LYP/DNP optimized geometry and dynamics of HEDA (white = hydrogen, blue=nitrogen, red = oxygen, gray = carbon). (a) image from the optimized geometry;(b) the isosurface plot of electronic density around atom in a molecule (isovalue = 0.015 a.u.)

Table 2 The softness and Fukui indices of the atoms in HEDA molecule calculated at the B3LYP/DNP by Hirschfeld population analysis.

| Atom | S | $f^-(r)$ | $s^-(r)$ |
|------|-------|----------|----------|
| 1O | | 0.036 | 0.171 |
| 4N | 4.742 | 0.211 | 1.000 |
| 7N | | 0.135 | 0.640 |

Conclusions

A series of novel thin-film HEDA/TMC composite membranes were successfully prepared from HEDA and TMC via interfacial polymerization. ATR-FTIR analysis confirmed the presence of the barrier layer on the porous substrate. SEM and AFM images also showed that the composite membranes possessed a compact structure. By increasing the concentration of HEDA from 0.3% to 0.5%, the resultant increase in degree of cross linking was found to improve the rejection ability of the membrane and decrease the permeate flux. Generally, the membrane showed the enhanced surface hydrophilicity due to the introduction of "off" groups, compared to the EDA based membranes. Among the TFC membrane series, the specific version X0.5Y0.1 exhibited optimum filtration performance, with permeate flux of 15.8 L/m² h and rejection of Na₂SO₄ (85.9%) and MgCl₂ (73.8%). Long term tests revealed that even after prolonged usage, the TFC membranes exhibited excellent durability and performance characteristics with a high permeate flux of 14.3 - 16.8 L/m²h and a negligible reduction of the salt rejection ability. Quantum mechanical simulation was employed to calculate the Fukui function by Hirshfield charge, and the values of global and local softness of the sites in the HEDA molecule within calculated density functional theory (DFT) were obtained. The results showed that the reactivity of 4N atom of HEDA monomer was much higher than that of the 1O and 7N atoms. This difference in reactivity is responsible for the loose structure in the initial stage and compact structure in the slow growth stage. The combined results indicate that these novel TFC membranes are promising candidates for future nanofiltration applications.

AUTHOR INFORMATION

Corresponding Author

Xuan Zhang (xuanzhang@mail.njust.edu.cn)

Lianjun Wang (wanglj@mail.njust.edu.cn)

Notes

The authors declare no competing financial interest.

Acknowledgment

This work was financially supported by the NSFC (21406117), the Natural Science Foundation of Jiangsu Province (BK20140782), National Science Foundation for Post-doctoral Scientists of China (2014M561652), the Jiangsu Planned Projects for Postdoctoral Research Funds (1401045B), Scientific Research Foundation for Returned Scholars (Ministry of Education of China), PAPD and the Fundamental Research Funds for the Central Universities (30920140122008, 30915011306).

Reference

1 M. A. Shannon, P. W. Bohn, M. Elimelech, J. G. Georgiadis, B. J. Marinas and A. M. Mayes, *Nature*, 2008, **452**, 301-310.

- 2 S. D. Kim, J. Cho, I. S. Kim, B. J. Vanderford and S. A. Snyder, *Water. Res.*, 2007, **41**, 1013-1021.
- 3 L. F. Greenlee, D. F. Lawler, B. D. Freeman, B. Marrot and P. Moulin, *Water. Res.*, 2009, **43**, 2317-2348.
- 4 M. Ulbricht, *Polymer*, 2006, **47**, 2217-2262.
- 5 E. M. Vrijenhoek, S. Hong and M. Elimelech, *J. Membr. Sci.*, 2001, **188**, 115-128.
- 6 R. Rohani, M. Hyland and D. Patterson, *J. Membr. Sci.*, 2011, **382**, 278-290.
- 7 H. Saitua, R. Gil and A. P. Padilla, *Desalination*, 2011, **274**, 1-6.
- 8 W. Fang, L. Shi and R. Wang, *J. Membr. Sci.*, 2013, **43**, 129-139.
- 9 Y. L. Lin, J. H. Chiou and C. H. Lee, *J. Hazard. Mater.*, 2014, **277**, 102-109.
- 10 T. Tsuru, S. Sasaki, T. Kamada, T. Shintani, T. Ohara, H. Nagasawa, K. Nishida, M. Kanezashi and T. Yoshioka, *J. Membr. Sci.*, 2013, **446**, 504-512.
- 11 H. Zhang, H. Mao, J. Wang, R. Ding, Z. Du, J. Liu and S. Cao, *J. Membr. Sci.*, 2014, **470**, 70-79.
- 12 H. Deng, Y. Xu, Q. Chen, X. Wei and B. Zhu, *J. Membr. Sci.*, 2011, **366**, 363-372.
- 13 M. F. Jimenez-Solomon, P. Gorgojo, M. Munoz-Ibanez and A. G. Livingston, *J. Membr. Sci.*, 2013, **448**, 102-113.
- 14 M. L. Sforça, I. V. P. Yoshida and S. P. Nunes, *J. Membr. Sci.*, 1999, **159**, 197-207.
- 15 X. Z. Wei, L. P. Zhu, H. Y. Deng, Y. Y. Xu, B. K. Zhu and Z. M. Huang, *J. Membr. Sci.*, 2008, **323**, 278-287.
- 16 M. F. J. Solomon, Y. Bhole and A. G. Livingston, *J. Membr. Sci.*, 2013, **434**, 193-203.
- 17 H. Q. Wu, B. B. Tang and P. Y. Wu, *J. Membr. Sci.*, 2013, **428**, 425-433.
- 18 A. Motohiro, T. Takahiro, B. Suaumu, M. Hidetoshi, T. Hiroki, T. Higashihara and M. Ueda, *J. Polym. Sci. A: Polym. Chem.*, 2014, **52**, 1275-1281.
- 19 B. Tang, Z. Huo and P. Wu, *J. Membr. Sci.*, 2008, **320**, 198-205.
- 20 J. Zhao, Y. Su, X. He, X. Zhao, Y. Li, R. Zhang and Z. Jiang, *J. Membr. Sci.*, 2014, **465**, 41-48.
- 21 J. Kaewsuk and G. T. Seo, *Desalin. Water. Treat.*, 2013, **516**, 218-6233.
- 22 R. Lo, A. Bhattacharya and B. Ganguly, *J. Membr. Sci.*, 2013, **436**, 90-96.
- 23 R. M. Gol, A. Bera, S. Banjo, B. Ganguly and S. K. Jewrajka, *J. Membr. Sci.*, 2014, **472**, 154-166.
- 24 A. E. Childress and M. Elimelech, *J. Membr. Sci.*, 1996, **119**, 253-268.
- 25 Y. C. Chiang, Y. Z. Hsub, R. C. Ruaan, C. J. Chuang and K. L. Tung, *J. Membr. Sci.*, 2009, **326**, 19-26.
- 26 J. Duan, E. Litwiller and I. Pinnau, *J. Membr. Sci.*, 2015, **473**, 157-164.
- 27 S. Yu, M. Ma, J. Liu, J. Tao, M. Liu and C. Gao, *J. Membr. Sci.*, 2011, **379**, 164-173.
- 28 V. Freger, *Langmuir*, 2003, **19**, 4791-4797.
- 29 L. M. Jin, S. L. Yu, W. X. Shi, X. S. Yi, N. Sun, Y. L. Ma and C. Ge, *Polymer*, 2012, **53**, 5295-5303.

- 30 S. Darvishmanesh, J. Degreve and B. V. D. Bruggen, *ChemPhysChem*, 2010, **11**, 404-411.
- 31 S. Darvishmanesh, J. Degreve and B. V. D. Bruggen, *Phys. Chem. Chem. Phys.*, 2010, **12**, 13333-13342.
- 32 T. Y. Liu, L. X. Bian, H. G. Yuan, B. Pang, Y. K. Lin, Y. Tong, B. Van der Bruggen and X. L. Wang, *J. Membr. Sci.*, 2015, **478**, 25-36.
- 33 Y. L. Ji, Q. F. An, Q. Zhao, H. L. Chen, C. J. Gao, *J. Membr. Sci.*, 2011, **376**, 254-265.
- 34 L. Li, S. Zhang and X. Zhang, *J. Membr. Sci.*, 2009, **335**, 133-139.
- 35 J. Liu, W. Yu, J. Zhang, S. Hu, L. You and G. Qiao, *Appl. Surf. Sci.*, 2010, **256**, 4729-4733.
- 36 P. D. Bernardo, A. Melchior, R. Portanova, M. Tolazzi and P. L. Zanonato, *Coordin. Chem. Rev.*, 2008, **252**, 1270-1285.
- 37 N. Iyi, H. Yamada, *Appl. Clay. Sci.*, 2012, **66**, 121-127.
- 38 D.R. Lide. *84th Handbook of Chemistry and Physics*, CRS Press, 2003, 1242.
- 39 J. Jegal, S. G. Min and K. H. Lee, *J. Appl. Polym. Sci.*, 2002, **86**, 2781-2787.
- 40 P. W. Morgan, Interfacial polymerization, in: K. Matyjaszewski, *Encyclopedia of Polymer Science and Technology*, John Wiley & Sons, Inc, 2011, pp 1-17.
- 41 E. L. Wittbecker and P. W. Morgan, *Interfacial polycondensation. I. J. Polym. Sci.*, 1959, **40**, 289-297.
- 42 P. W. Morgan and S. L. *J. Polym. Sci. A*, 1996, **34**, 531-559.